Three Dimensional High-Resolution Simulations of Richtmyer-Meshkov Mixing and Shock-Turbulence Interaction

R. H. Cohen[1], W. P. Dannevik[1], A. M. Dimits [1], D. E. Eliason[1], A. A. Mirin[1], D. H. Porter[2], O. Schilling[1], and P. R. Woodward[2]
[1]Lawrence Livermore National Laboratory
P.O. Box 808, Livermore CA 94550 USA
[2]Astronomy Department, University of Minnesota
Minneapolis, MN 55455 USA

Abstract: Three-dimensional high-resolution simulations are performed of the Richtmyer-Meshkov (RM) instability for a Mach 6 shock, and of the passage of a second shock from the same side through a developed RM instability. The second shock is found to rapidly smear fine structure and strongly enhance mixing. Studies of the interaction of moderately strong shocks with a pre-existing turbulent field indicate amplification of transverse vorticity and reduction of stream-wise vorticity, as well as the mechanisms for these changes.

1. Introduction

The Richtmyer-Meshkov (RM) instability [1] is the impulsive-acceleration limit of the Rayleigh-Taylor (RT) instability, and occurs, for example, when a shock passes through an interface of two fluids of differing density. We report here preliminary results from three-dimensional high-resolution direct numerical simulations (DNS) using the piecewise-parabolic method (PPM)[2]. We study the effects of a second shock both directly and via simulations of the passage of a shock through a pre-existing turbulent field. These simulations, and our companion RT simulations, [3] represent one component (generation of benchmark DNS data sets) of a larger project to develop validated sub-grid-scale models for large-eddy compressible simulations, part of the U.S. Department of Energy's Accelerated Strategic Computing Initiative (ASCI).

Three-dimensional high-resolution hydrodynamics computations have been limited by available computer resources. While some low-resolution studies of RM instability (*e.g.*, [4]-[6]) and shock-turbulence interaction [7] have appeared, studies exceeding 10^6 computational zones are only now becoming available; see for example [8].

A recent experimental study [9] of 2-D incompressible fluids indicates dramatically the effect of subjecting developed RM turbulence through a second impulsive acceleration in the same direction as the first. The second event rapidly scrambles the bubble-and-spike structure and enhances the mixing. A natural question is, is there a comparably dramatic effect in 3D and with compressible fluids?

2. Richtmyer-Meshkov Simulations

Our simulations are done with a single fluid plus a passive scalar field to monitor mix. The pre-shock gas is initialized with constant pressure and a 2x density contrast on either side of a perturbed planar interface (at stream-wise coordinate $z = 0.5$). The interface perturbation

[0]Email contact: rcohen@llnl.gov

is either a product of single sinusoidal components in the horizontal (x and y) directions, or a set of 32^2 modes with a $k^2 \exp(-k^2/k_0^2)$ distribution of amplitudes and random phases and a mode width k_0 corresponding to 8 wavelengths per unit length. This gas impinges on a higher-density, higher-pressure gas to initiate a Mach 6 shock on the low-density side of the contact discontinuity. Boundary conditions are periodic in x and y and continuation (zero derivative) in z. Most of the shock is absorbed at the z boundary, though a weak wave is reflected; this can be eliminated with additional computational cost. The passive scalar is initialized with two constant values (color-coded red and blue in the color plates; the light fluid is blue) on either side of the initial contact discontinuity.

Plate 1 shows the passive scalar field at $t = 3$, where time is measured in units of a nominal box length over the pre-shock sound speed in the gas on the lower-density side of the contact discontinuity. The initial surface deformation is the random-phase model with amplitude 0.02 RMS. The resolution is 256^3, the Navier-Stokes viscosity is 4×10^{-5} and the Prandtl number is 1. Our experience with Rayleigh-Taylor simulation at this viscosity and several resolutions indicates that this simulation is resolved. The largest (in z) features tend to correlate with large features in the initial perturbation, consistent with prior observations of persistence of initial conditions. Also compared to the corresponding RT visualization at comparable parameters, [3], even though the initial condition for our RM simulation is slanted more toward longer wavelengths. The growth of the RM mixing layer (measured by where the horizontal average of the passive scalar is 0.1 and 0.9) is as shown in Fig. 1a; the fit is of the form $\Delta z = c(t + t_0)^p$ with $p = 0.75$, $t_0 = 0.175$, and $c = 0.33$. That the asymptotic behavior is a power law with $p < 1$ is in agreement with the conclusions of Refs. [8], [10], and [11].

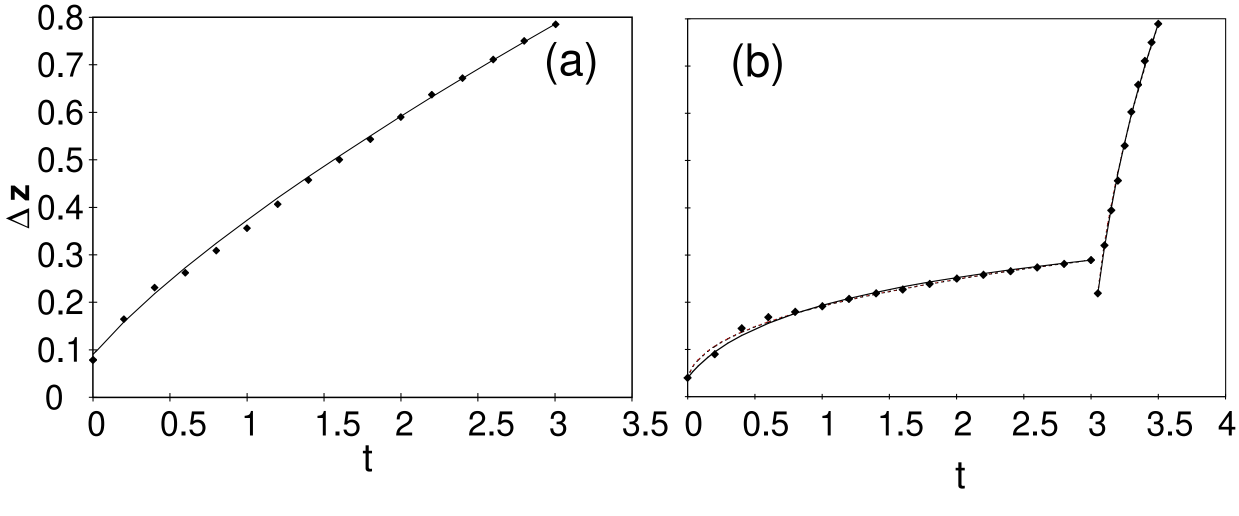

Figure 1. Mixing layer growth vs. time for (a) random-phase sum initial condition; (b) single mode initial condition with two shocks

Plate 2 shows the corresponding result for a single sine-wave perturbation with wavelength 1/2 the box width of the random-phase simulation. The resolution of $128^2 \times 288$ (not all shown) yields a resolved Navier-Stokes simulation. The development of fine-scale, non-chaotic features is evident. The growth of the mixing layer (measured by departure of the passive scalar from its initial values) is indicated by the $t < 3$ portion of Fig. 1b. The fit represented by the solid curve is asymptotically logarithmic as expected for a single bubble and spike, $\Delta z = \Delta z_0 + c_1 \ln(1 + at)$, with $c_1 = 0.010$, $\Delta z_0 = 0.04$, and $a = 3.5$. Actually a slightly better fit is obtained by a power-law form (dotted curve) $c_p(t + t_0)^p$ with $p = 0.38$, $t_0 = 0.0165$ and $c_p = 0.19$.

Plate 3 depicts the result of passing an additional Mach 6 shock through the interface from the same (low-density) side. Even at $t = 3.1$ (not shown), there is a distinct change in character, with much of the fine structure smeared out. In the time slice shown, at $t = 3.2$, we additionally see the beginning of an inversion in the near corner of the simulation; what had been a spike of red fluid extending into blue begins to detach while blue fluid encroaches on red around the edges of the spike. At later times ($t \sim 3.3 - 3.5$) the red spike detaches and a jet of blue penetrates (rapidly) through the former red region. The second shock significantly accelerates mixing-region growth following an initial contraction, as can be seen from the right-hand portion of Fig. 1b. Equally good (almost indistinguishable) fits of logarithmic (dotted) and power-law forms are obtained: respectively, $\Delta z_0 + c_l \ln[1 + b(t - t_0)]$ with $\Delta z_0 = 0.22$, $t_0 = 3.2$, $c_l = 0.61$, and $b = 3.5$; and $c_p(t + t_0)^p$, with $p = 0.55$, $t_0 = -3.0$, and $c_p = 0.42$ The rapid destruction of features and acceleration of mixing is reminiscent of the experimental results in Ref. [9]; though in our case, some, but not all, of the acceleration is due to the increased sound speed (factor of about 4) following the second shock.

3. Shock-Turbulence Interaction

We also perform simulations of the interaction of a shock with a pre-existing turbulent field. These may be viewed as providing a view of second-shock interaction on the more microscopic scale of the secondary instabilities arising in the nonlinear stages of the RM instability. A random-phase Gaussian-distributed spectrum of 8^3 modes is allowed to decay from a turbulent Mach number of 0.75 to about 0.2. Then a shock is induced by specifying inflow boundary conditions corresponding to the desired down-stream (quiescent) gas. These simulations are done with only the dissipation provided by the PPM algorithm. The resulting x vorticity field for a Mach 6 shock in a 512^3 resolution simulation is shown in Plate 4. We observe a significant amplification induced by the shock passage. The shock itself is not directly visible, but is at the right edge of the amplified region. The dark region on the left is the high-density quiescent gas introduced to generate the shock. There is considerable distortion of the shock front, but comparison with a turbulence-free run shows no measurable change in propagation speed.

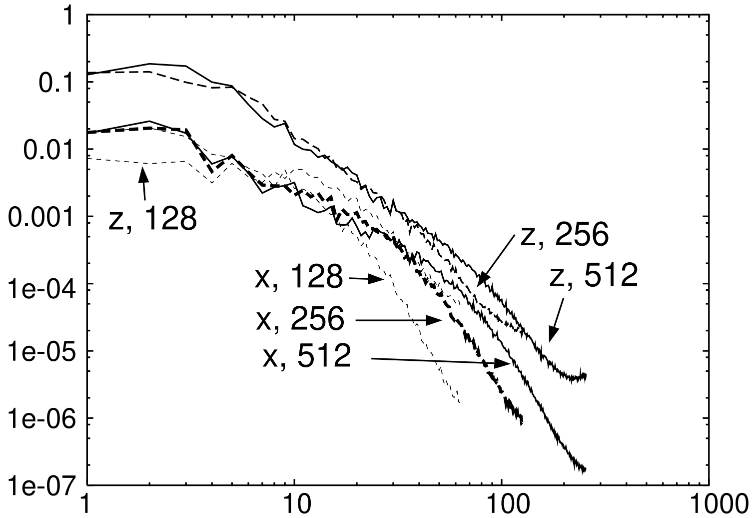

Figure 2. x and z velocity power spectra at 128^3, 256^3, and 512^3 resolution

Velocity power spectra (power per unit-thickness annulus in k_x, k_y space) are shown in Fig. 2 for several resolutions. These spectra suggest that a meaningful inertial range is present in the 256^3 and 512^3 simulations, and that the results at 256^3 and 512^3 are converged in the energy containing range and the captured portion of the inertial range. They also indicate a steepening of the v_z spectrum relative to v_x. The v_x spectrum is approximately the same shape as that of all components in the unshocked gas (not shown), with a Kolmogorov-type $k^{-5/3}$ slope in the inertial range, but overall larger. The vorticity component ω_j spectra show a similar convergence, and a steepening of ω_x relative to ω_z.

Figure 3a shows ω_j as a function of z. Evident features are the amplification of the ω_x (and ω_y), and the smaller reduction in the ω_z, and the re-isotropization further down stream. Still further down stream, all components drop off as the quiescent gas region is entered. The amplification of ω_x, ω_y and the reduction of ω_z have a smooth variation with Mach number, as shown in Fig. 4 for a series of 256^3 simulations. The relative changes are approximately characterized by: $\Delta\omega_j/\omega_j \approx C_j\,(M-1)^{0.6}$, with $C_x \approx C_y \approx 0.38$, and $C_z \approx -0.099$.

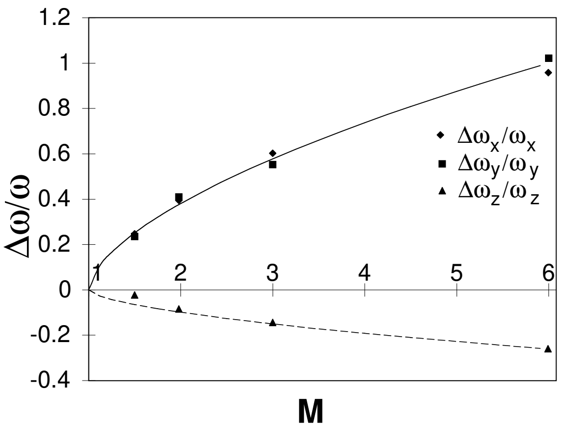

Figure 4. Relative change in vorticity vs. shock Mach number

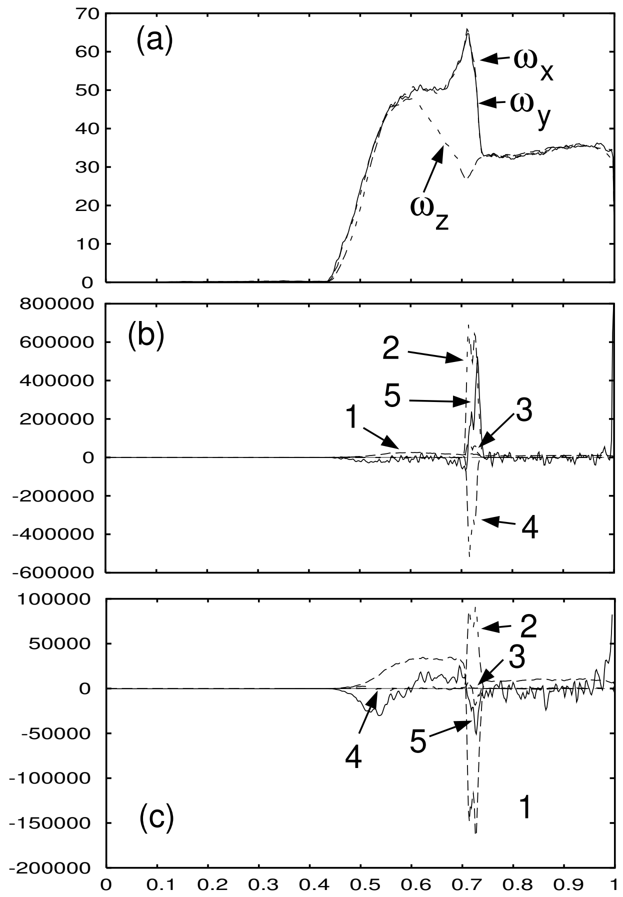

Figure 3. Vorticity component evolution: (a) r.m.s. vorticities vs. z; (b) terms in x enstrophy equation; (c) terms in z enstrophy equation

In order to identify the mechanisms responsible for the observed effects, we separately evaluate and plot each term in the equation of evolution for the horizontal averages of squares of the vorticity components ("enstrophy components"), which we write in the form:

$$\begin{aligned}\frac{\partial\left\langle\omega_j^2/2\right\rangle}{\partial t} &+ \langle\mathbf{v}\rangle\cdot\nabla\left\langle\omega_j^2/2\right\rangle \approx \mathbf{v}^*\cdot\nabla\left\langle\omega_j^2/2\right\rangle \\ &= \langle\omega_i(\omega\cdot\nabla)v_i\rangle - \left\langle\omega_j^2\nabla\cdot\mathbf{v}\right\rangle + \left\langle(\omega/\rho^2)\cdot\nabla\rho\times\nabla P\right\rangle - \left\langle\mathbf{v}'\cdot\nabla\omega_j^2/2\right\rangle\end{aligned}$$

where $\mathbf{v}^*$ is the average velocity in a reference frame in which the shock is at rest and $\mathbf{v}' = \mathbf{v} - \langle\mathbf{v}\rangle$. The terms on the right hand side are, respectively, vortex stretching, enstrophy dilatation, baroclinic production, and nonlinear advection. These terms are separately plotted along with $\mathbf{v}^* \cdot \nabla\omega_j^2$ in Fig. 3b and 3c. We observe that the increase in ω_x (and ω_y) is primarily the result of dilatation, while the decrease in ω_z and its subsequent recovery results mainly from vortex stretching. There is a significant contribution from the nonlinear advection term, implying that conventional rapid distortion theory or linear interaction analysis, which would neglect it, would not provide an accurate answer.

4. Discussion and conclusions

In addition to reproducing familiar features of the Richtmyer-Meshkov instability, we have found smearing of fine-scale structure and rapid mixing caused by the passage of a second shock in the same direction, similar to that observed experimentally [9] for incompressible fluids, as well as detachment of spikes. We find a weaker departure from linear growth of the mixing layer for our random sum of modes than for a single mode, and for the mixing following the second shock than after the initial shock.

For the interaction of a shock with pre-existing turbulence, we find overall amplification of vorticity by the passage of a shock, as has been noted and quantified previously [7] for the case of a weak shock. However, Ref. [7] reports change in only the transverse vorticity, and finds negligible contribution from nonlinear advection and hence good agreement with a linear interaction analysis. Here we study moderately strong shocks, find that there is an opposing change in the stream-wise component ω_z, and observe that while the increase in ω_x (and ω_y) is due primarily to the compressibility term, there is an important contribution from nonlinear advection. We also find a decrease and subsequent recovery of ω_z, both resulting from vortex stretching. The overall increase in the ω^2 can be viewed as the stirring process that breaks up the fine structure when a second shock passes through a developed Richtmyer-Meshkov instability. The observed asymmetry in which vorticity components normal to the shock propagation are amplified while that in the shock propagation direction decreases implies selectivity in the *kinds* of fine-scale features broken up.

Acknowledgement. Work performed under for the U.S. Department of Energy at Lawrence Livermore National Laboratory and at University of Minnesota under Contract W7405-ENG-48. Computations performed in part on the ASCI Blue Pacific IBM SP system.

References

[1] Richtmyer, R.D., Comm. Pure and Applied Math **13**, 297 (1960), and Meshkov, E.E., Isv. akad. Nauk SSR, Mekhanika Zhidkosti i Gaza, n.5, 151 (1969).
[2] Woodward, P.R. and Collela, P., J. Comp. Phys. **54**, 174 (1984).
[3] Schilling, O., Cohen, R.H., Dannevik, W.P., *et al.*, this volume.
[4] Cloutman, L.D. and Wehner, M.F., Phys. Fluids A **4**, 1821 (1992).
[5] Demchenko, V.V., in *Compressible Turbulent Mixing*, R. Young, J. Glimm and B. Boston, eds. (World Scientific, Singapore, 1996) p. 331.
[6] Lebo, I.G., Rozanov, V.B., Tishkin, V.F., *et al.*, *ibid*, p. 346.
[7] S. Lee, S. Lele and P. Moin, J. Fl. Mech **251**, 533 (1993)
[8] Youngs, D.L., Laser and Particle Beams **12**, 725 (1994).
[9] Jacobs, J.W., and Sheeley, J.M., Phys. Fluids bf 8, 405 (1996).
[10] Barenblatt, G.I., in *Non-linear Dynamics and Turbulence*, G.I. Barenblatt, G. Loos, and D.D. Joseph, eds. (Pitman, Boston, 1983).

[11] Neuvazhayev, V. Ye., Matematicheskoye Modelinovaniye **3**, 10 (1991).

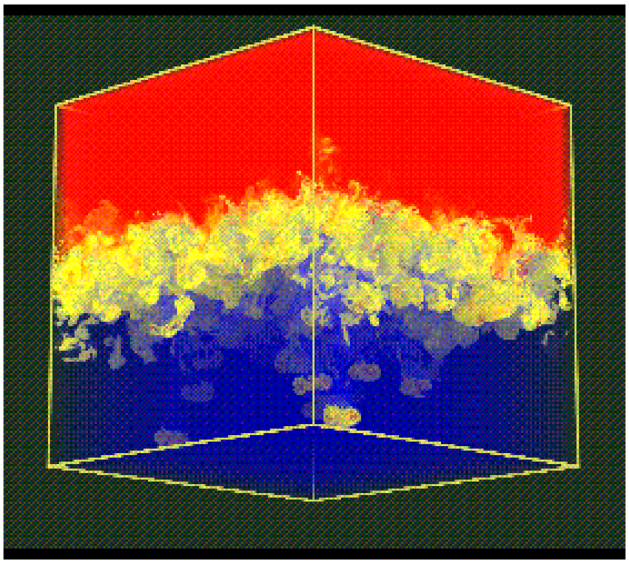

Plate 1: Passive scalar field at t=3 for random-phase sum initial condition

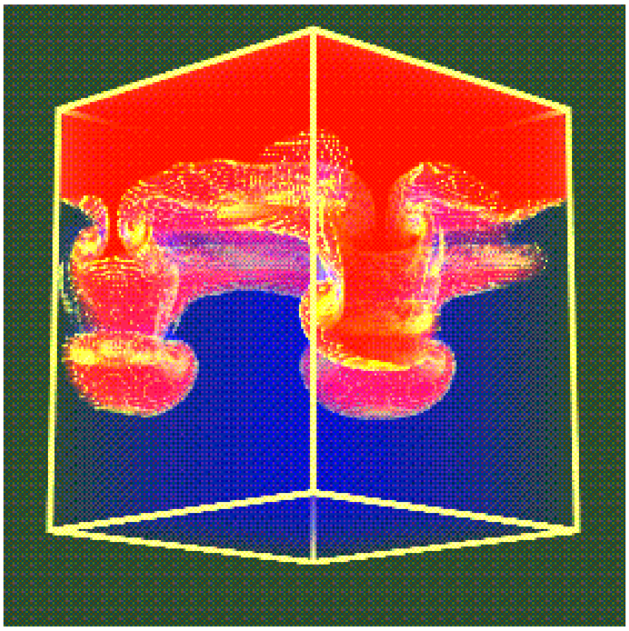

Plate 2: Passive scalar field at t=3 for single-mode initial condition, just before second shock

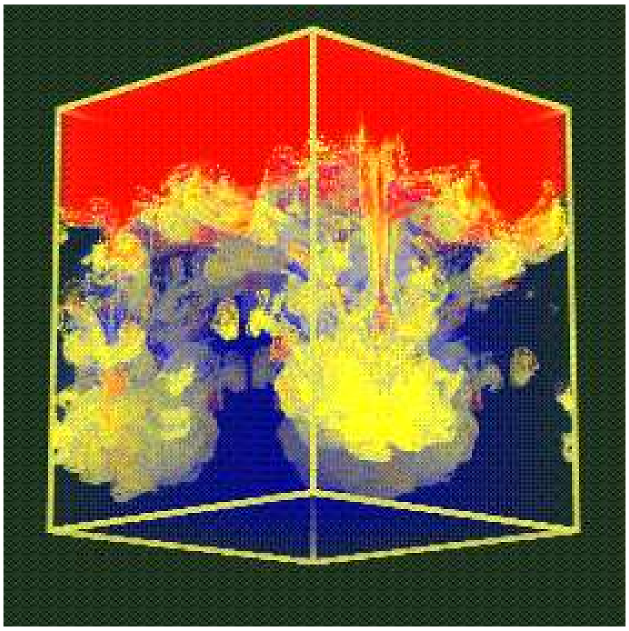

Plate 3: Passive scalar field at t=3.2 for single-mode initial condition, after second shock

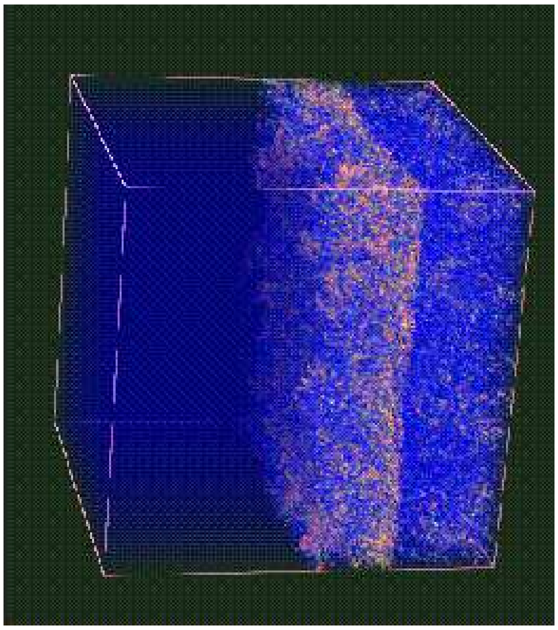

Plate 4: Magnitude of x vorticity for shock-turbulence interaction